ISSN 1069-3513, Izvestiya, Physics of the Solid Earth, 2013, Vol. 49, No. 4, pp. 577–586. © Pleiades Publishing, Ltd., 2013.
Original Russian Text © G.N. Kopylova, L.N. Taranova, 2013, published in Fizika Zemli, 2013, No. 4, pp. 135–144.

Synchronization Signals in the Variations of Groundwater Chemical Composition in Kamchatka in Relation to the Strong ($M_w \geq 6.6$) Earthquakes

G. N. Kopylova and L. N. Taranova

Kamchatka Branch of the Geophysical Survey, Russian Academy of Sciences, bulv. Piip 9, Petropavlovsk-Kamchatskii, 683006 Russia

Received July 25, 2012; in final form, November 22, 2012

Abstract—We consider the results of the statistical analysis using the methods of the principal components and canonical coherences applied to the processing of long (1986–2005) time series of hydrogeochemical observations at the flowing wells and springs in Kamchatka. The time-frequency diagrams of the evolution of informative statistics characterizing the collective behavior of multidimensional hydrogeochemical time series are constructed, and the time intervals and frequency bands where the *synchronization signals* (Lyubushin, 2007) appear are identified. The features of their occurrence are analyzed in comparison to the strong ($M_w = 6.6–7.8$) local earthquakes. It is found that such signals in the measurements of some multidimensional time series can arise both before and after earthquakes, i.e. these signals have a precursory (P2) and postseismic (P3) character.

DOI: 10.1134/S106935131304006X

INTRODUCTION

Studying the precursors of the earthquakes and creating the intermediate-term seismic forecasts on this basis are issues of vital importance for conducting complex geophysical, geochemical, and strainmeter observations in seismically active regions (Sobolev, 1993). These observations provide the time series of various parameters characterizing the electromagnetic and other fields of the Earth, the groundwater dynamics, and strain parameters, whose variations may contain the signs of the impending seismic catastrophe. However, despite many years of research in this direction, the questions concerning identifying, classifying, and estimating the reliability for various types of precursors, as well as developing the governing principles of the decision (i.e., when to issue the alarms), are mainly the subject of scientific discussions.

In the Kamchatka region, the intermediate-term seismic hazard assessment with an advance time from a few years to a few months and weeks typically relies on the expert analysis of the observation data (Chebrov et al., 2011.) The key elements of the expert analysis are the regular reports on the separate types of observations based on the current data on the particular types of precursors and their comparison with the retrospective experience in observing these effects in relation to the earthquakes. According to the data of (Kopylova and Serafimova, 2009; Serafimova and Kopylova, 2010; Chebrov et al., 2011), in the Kamchatka region, the precursors in the individual types of observations and in their complex appear within a few weeks and months before the earthquakes with magnitudes of at least 6–7 at a distance of a few hundred km.

The hydrogeochemical observations of the groundwater and gas composition are one of the methods of searching for precursors of earthquakes. In Kamchatka, such observations are conducted by the Kamchatka Branch of the Geophysical Survey, Russian Academy of Science (KB GS RAS) on the network of flowing wells and springs (Kopylova et al., 1994; Khatkevich and Ryabinin, 2004). These studies provide long time series of the variations in the concentrations of the dissolved minerals and gases in the composition of the groundwater with the periodicity of three days. Such time series for each particular source are multidimensional since they include the data on the analytically determined main cations and anions, dissolved gases, nondissociated molecules such as boric and silicic acids, as well as the physicochemical parameters: the discharge, water temperature, and pH. Therefore, the number of the time series for a single water source may reach a few dozens (10–20).

In some of the time series of hydro-geochemical observations, visual analysis has retrospectively revealed anomalous variations correlated to several strong earthquakes (Kopylova et al., 1994; Khatkevich and Ryabinin, 2004; Kopylova, 2010). By the time of their appearance relative to the occurrence of earthquakes with magnitudes of about 7 and higher, these anomalies are classified into hydrogeochemical precursors and postseismic effects. The precursory variations related to the Kamchatka earthquakes of October 6, 1987 ($M_w = 6.6$), March 2, 1992 ($M_w = 6.9$) were

observed in the changes of the chloride ion concentration in the GK-1 borehole and in the changes of the concentration of hydrogen carbonate ion, sulfate ion, sodium, and calcium in the water of the Moroznaya-1 well (Kopylova et al., 1994; Kopylova and Boldina, 2012). At the same time, variations in a number of other hydrogeochemical characteristics of groundwater composition did not show any precursory anomalies or showed much weaker anomalies. In our opinion, this was mainly due to the inaccurate analytical determination of most of the mineral components in the groundwater composition, which, correspondingly, made it impossible to distinguish the signal against the noise variations in separate one-dimensional time series by visual examination.

The application of the statistical method for processing the multidimensional time series by estimating the maximal eigenvalues of spectral matrices and the statistics of canonical coherences in a moving time window (Lyubushin, 1993; 1994; 1998; 2007) is aimed at revealing the most prominent characteristic features in the joint variations of a set of the parameters, and, in particular, the hydrogeochemical data. The suggested method is a means of reducing the dimensionality of the multidimensional data (to which the hydrogeochemical data are related); it can provide a qualitatively new data representation in the form of frequency-time diagrams reflecting the evolution of the informative statistics with the routine expert approach to forecasting earthquakes.

By constructing the frequency-time diagrams of the evolution of the informative statistics, which describe the most general features in the behavior of the multidimensional hydrogeochemical time series, one can reveal the *synchronization signals* (Lyubushin, 2007) by the increase in the amplitudes of these diagrams and assess the time intervals and frequency bands of their occurrence. The *synchronization signals* are formalized (informationally-mathematical) images of the increased coherence in the joint variations of the individual time series of hydrogeochemical observations; these signals can serve as the markers of increased coupling between these factors during the preparatory stages of strong earthquakes.

The efficiency of the methods of the principle components and canonical coherences in revealing the synchronization signals in the variations of multidimensional time series of hydrogeochemical data during the preparatory stages of the Kamchatka earthquakes of 1987 and 1992 with magnitudes of 6.6 and 6.9, respectively, was demonstrated in (Lyubushin et al., 1996; 1998; Lyubushin, 1998). In relation to these earthquakes, three types of the synchronization signals were identified. By the time of their appearance relative to the occurrence of the earthquakes, these signals are classified into the precursory (P2) and postseismic (P3) effects; in addition, the variations in some multidimensional time series were also found to contain a synchronization signal that corresponds to the sequential appearance of precursory and postseismic changes (P2 + P3). In fact, type P2 synchronization signals in the variations of a complex of hydrogeochemical parameters should be considered as a new synthetic hydrogeochemical precursor suitable for use in the practice of earthquake forecasting with due assessment of its reliability and seismoprognostic efficiency.

In 1992–1999, Kamchatka experienced an increased seismic activity and was hit by eight earthquakes with M_w = 6.9–7.8, including the strongest Kronotskoe earthquake on December 5, 1997 (M_w = 7.8), which was preceded by intermediate-term precursors in the variations of seismological, deformational, and hydrogeological parameters (Kopylova and Serafimova, 2009; Serafimova and Kopylova, 2010). Therefore, retrospective estimation of the synchronization signals in the variations of multidimensional hydrogeochemical data during a long period that included a few strong seismic events is of interest for designing the methods for processing and interpretation of the hydrogeochemical observations, which are focused on the detection of precursors of strong earthquakes in Kamchatka.

In this paper, we present the results of processing the time series of concentrations of chloride ion (Cl^-), hydrogen carbonate ion $\left(HCO_3^-\right)$, and dissolved silica acid (H_4SiO_4) in the water in the GK-1 well (hereinafter, GK1) and springs 1 (I1) and 2 (I2) at the Pinachevo site, and well 1 at the Moroznaya site (M1) over the 15-year interval from 1986 to 2001. Some of the processed multidimensional time series have a duration of 19 years (1986–2005). The characteristic of the wells and springs and the description of the observation method are presented in (Kopylova et al., 1994; Khatkevich and Ryabinin, 2004).

The layout of the observation sites and the epicenters of 11 earthquakes with M_w = 6.6–7.8 (table) that occurred in 1987–2004 is shown in Fig. 1. It is assumed that the preparatory processes of these earthquakes could have controlled the collective changes in the hydrogeochemical parameters characterizing the groundwater regime. Additional support for this assumption is provided by the precursory anomalies recorded before these earthquakes not only in the changes of individual time series of the hydrogeochemical data but also in the water level variations and a number of seismological and deformational parameters. Particularly striking anomalies in a wide set of parameters preceded earthquakes 1, 2, and 7 (Kopylova and Serafimova, 2009; Serafimova and Kopylova, 2010).

Figure 2a shows the cumulative graph of seismic energy released by the earthquakes with $M_w \geq 5.0$ in the depth interval from the surface to 250 km within 400 km of Petropavlovsk-Kamchatskii. This graph characterizes the seismic regime in the Kamchatka seismic zone during the interval from 1986 to 2005.

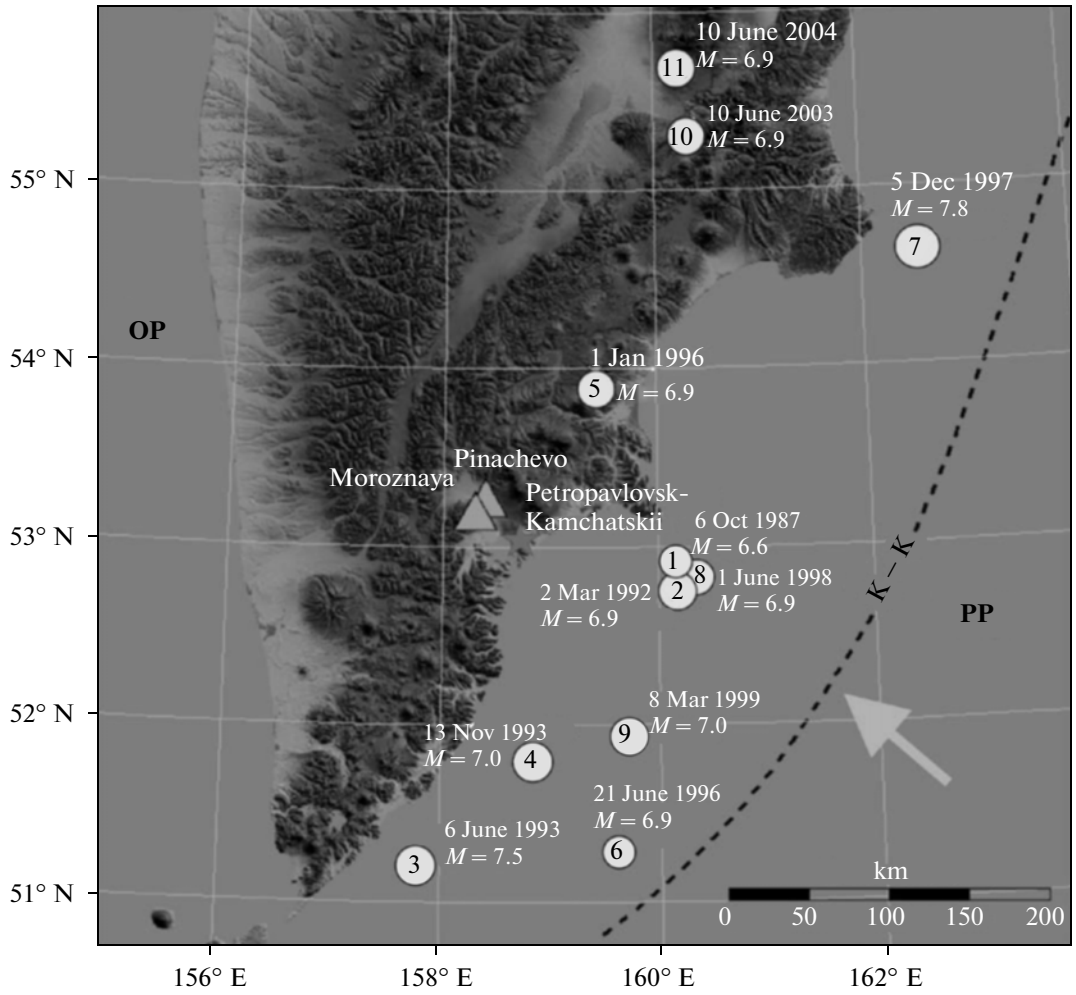

Fig. 1. The layout of the observation sites (the triangles) and the epicenters of the earthquakes with $M_w \geq 6.6$ occurred in 1987–2004 (the circles). PP is the Pacific oceanic plate, OP is the Okhotsk continental plate, and K–K is the Kuril–Kamchatka deep trench. The arrow shows the direction of motion of PP.

Figure 2b depicts the time distribution of the earthquakes with $M \geq 5.0$. It is seen that the eleven seismic events considered in our analysis (Fig. 1, table) distinctly manifest themselves by the steps in the cumulative graph (Fig. 2a), and more than 90% of the energy of the elastic seismic waves was released by these earthquakes.

In order to qualitatively compare the efficiency of individual earthquakes in controlling the groundwater dynamics of the wells and springs, the ratio $M_w/\log R$, where R is the average epicentral distance to the groundwater monitoring sites in km, is presented in the table for each earthquake.

THE PROCEDURE OF DATA PROCESSING

Figure 3 shows the time series of the observations at GK1, S1, S2, and M1 against the time of occurrence of the earthquakes (table). Consider the most prominent features in their variations during the periods of strong earthquakes, which are revealed by the visual analysis of separate one-dimensional time series and described previously in (Kopylova et al., 1994; Kopylova and Boldina, 2012; Khatkevich and Ryabinin, 2004).

In the water regime of the GK1 well, the hydrogeoseismic variations, i.e., the changes in the parameters of the hydrogeological regime caused by the preparatory phenomena and the occurrence of some earthquakes, are traced by the opposite-phase changes in the chloride-ion concentration, which decreases before and increases after the earthquakes, and hydrogen-carbonate-ion concentration, which increases before and decreases after the earthquakes. These changes were observed in relation to earthquakes 2–4 and 7. The variations in the concentration of silicic acid do not show any regular variations correlated to the earthquakes.

The gradual growth in the concentrations of chloride ions and hydrogen-carbonate ions after the strong

The data on the earthquakes with $M_w \geq 6.6$ occurred in 1987–2004 (according to the KB GS RAS, Geophysical Survey of RAS, and NEIC)

No.	Date, yyyymmdd	Time, hh:mm	Latitude, deg. N	Longitude, deg. E	Depth, km	Class, *Ks*	Epicentral distance, *R*, km	M_w	MSK64 intensity at PET	$M_w/\log R$	Days from January 4, 1986
1	19871006	20:12	52.86	160.23	33	14.1	130	6.6	4–5	3.12	641
2	19920302	12:30	52.76	160.20	20	14.6	130	6.9	5–6	3.26	2250
3	19930608	13:04	51.20	157.80	40	15.0	230	7.5	5	3.18	2713
4	19931113	01:18	51.79	158.83	40	14.6	160	7.0	5–6	3.18	2871
5	19960101	09:58	53.88	159.44	0	14.3	100	6.9	4–5	3.45	3650
6	19960621	13:57	51.27	159.63	2	13.9	230	7.0	3–5	2.96	3822
7	19971205	11:27	54.64	162.55	10	15.5	200	7.8	5–6	3.39	4354
8	19980601	05:34	52.81	160.37	31	13.8	140	6.9	4–5	3.22	4532
9	19990308	12:26	51.93	159.72	7	14.3	170	7.0	4–6	3.14	4812
10	20030616	22:08	55.30	160.34	190	14.7	260	6.9	3–4	2.86	6373
11	20040610	15:20	55.68	160.25	208	14.9	300	6.9	3–4	2.78	6733

Note: PET stands for Petropavlovsk-Kamchatskii.

earthquakes, which are followed by their subsequent long-lasting decay, are the most prominent features of the water dynamics on springs 1 and 2. The postseismic effects in the variations of the concentration of the silicic acid are less common.

In the M1 well, the hydrogeoseismic variations preceding and accompanying earthquakes 1–5 appeared as decreases in the hydrogen carbonate ion concentration. Regular variations in the silicic acid concentration associated with strong earthquakes have not been identified.

The visual analysis of the primary data shows that the changes in the separate data series before and during strong earthquakes are individual and specific to each particular water source. Only the regular postseismic effects in the variations of chloride-ion and hydrogen-carbonate-ion concentrations in the water of springs 1 and 2 are the exception. These peculiarities in the formation of the hydrogeochemical dynamics of the groundwater cause some difficulties in the interpretation of the hydrogeochemical data for premonitory signs of strong earthquakes.

Using the time series shown in Fig. 3, we have formed eight multidimensional series of hydrogeochemical data, each including at least three simul-

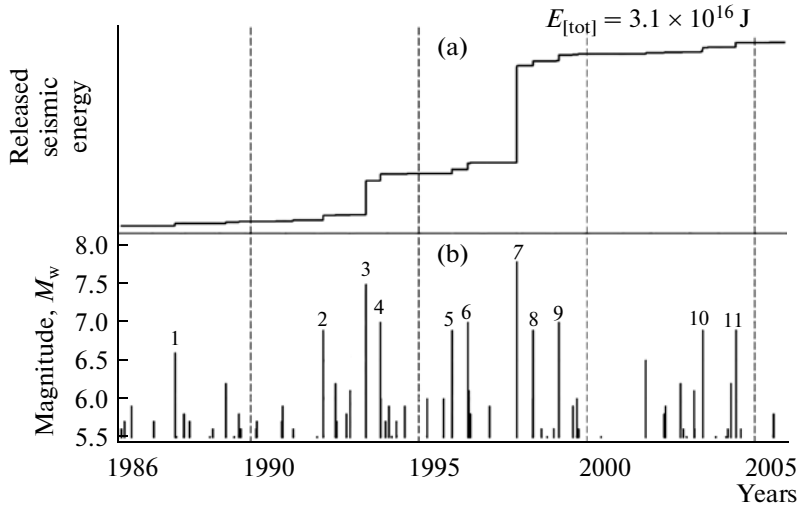

Fig. 2. The characteristics of seismic regime in Kamchatka in 1986–2005. (a) is the cumulative graph of seismic energy release by the earthquakes with $M_w \geq 5.0$ within 400 km of Petropavlovsk-Kamchatskii (53.0° N, 158.6° E) at the depth from 0 to 250 km. (b) is the time distribution of the earthquakes with $M_w \geq 5.0$; the numbers of earthquakes correspond to their numbers in the table and Fig. 1.

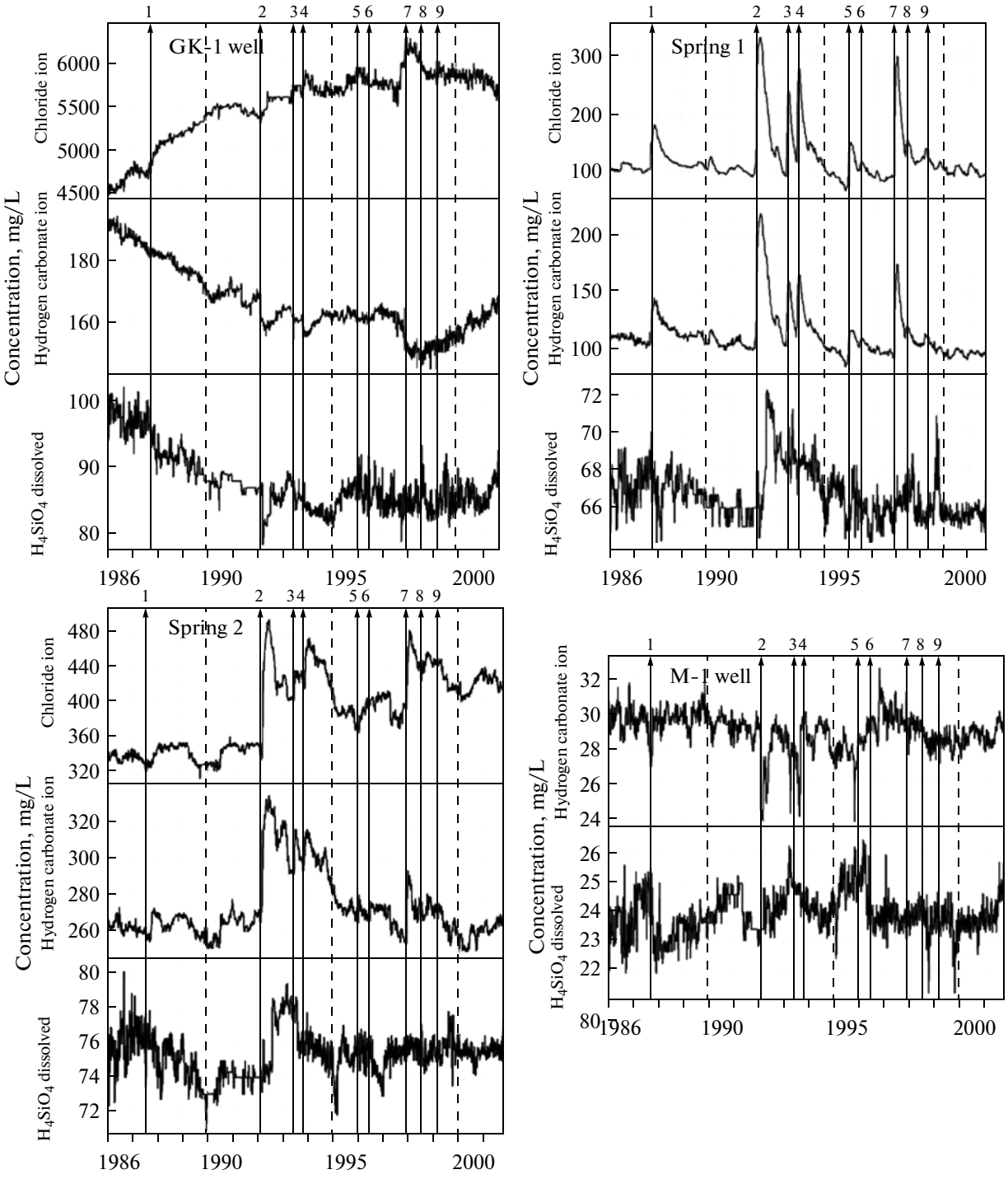

Fig. 3. The changes in the parameters of hydrogeochemical regime of wells and springs in 1986–2001 in comparison to the occurrence time of the earthquakes. The numbers of the earthquakes correspond to their numbers in the table and Figs. 1 and 2.

taneous time series ($n \geq 3$, where n is the number of 1D time series that compose the multidimensional series).

The entire set of the formed multidimensional series is classified in three groups (I–III).

Group I is composed of multidimensional series formed from one-dimensional hydro-geochemical series for separate water sources. For the S1 and S2 springs and GK1 well, one three-dimensional series was formed for each of these sources (S1_3, S2_3, and GK1_3).

The multidimensional series of Group II include the data for separate hydrogeochemical parameters measured at several ($n \geq 3$) sources. In the analytical determinations of concentration, each component in

the groundwater composition has its own individual accuracy (Khatkevich and Ryabinin, 2004) and, as shown above, the source-specific individual pattern of changes related to the earthquakes. Therefore, the analysis of the three multidimensional series of group II (Cl_3, HCO3_4, and H4SiO4_4) is aimed at assessing the informative content of different hydrogeochemical parameters and tracing the peculiarities in their collective behavior that are associated with earthquakes.

Group III comprises the time series of concentrations for different chemical components of the groundwater from several sources. For example, the data observed at the GK1, S1, and S2 sources of the Pinachevo site form the 9-dimensional series (III_9); the observations at the GK1, M1, S1, and S2 compose a 11-dimensional series (III_11) (Fig. 3).

For each initial time series (Fig. 3), we used the increments in order to suppress the trends and intense low-frequency components in these measurements (Lyubushin, 1993; 2007; Lyubushin et al., 1996; 1997).

With a three-day interval of data discretization, it is possible to study variations in the hydrogeochemical parameters at the frequencies ranging from 1/6 day^{-1} = 0.167 day^{-1} to $1/L$, where L is the length of the moving time window. In this study, we analyzed the frequency band from 1/6 day^{-1} to $5/L$ day^{-1}; thus, the length of the moving time window is the size of at least five wavelengths of the lowest-frequency variations. Assuming the window to have a length of 100 and 200 counts, or 300 and 600 days, we obtain the target frequency interval ranging from 1/6 to 1/60 and 1/120 day^{-1} (0.1667–0.0167 day^{-1} and 0.1667–0.0083 day^{-1}).

The duration of most of the previously revealed hydrogeochemical precursors ranges from the first few months to 7–9 months (Kopylova, 2010; Kopylova et al., 1994; Khatkevich and Ryabinin, 2004). The duration of postseismic variations is approximately of the same order of magnitude. Therefore, a time window with a length of 100 and 200 counts (300 and 600 days) shifted with a step of 10–20 counts (30–60 days) appears to be quite reasonable from the standpoint of revealing relatively high-frequency synchronization signals in the collective variations of the groundwater chemical composition.

According to the mathematical algorithms described in (Lyubushin, 1993; 1998; 2007), we carried out the calculations and constructed the frequency-time diagrams for the evolution of three statistics:

(1) the maximal eigenvalue of spectral matrix $\lambda_1(\tau, \omega)$, where τ is the right end of the moving time window and ω is frequency;

(2) the sum of the squared componentwise canonical coherences $\rho^2(\tau, \omega)$;

(3) the product of the componentwise canonical coherences $\kappa(\tau, \omega)$.

From a computational standpoint, the quantity $\lambda_1(\tau, \omega)$ is a power spectrum of the first principal component of a multidimensional series, i.e., a certain scalar time series obtained by linear filtering of a multidimensional series. This quantity carries the maximum information about the joint (synchronous) behavior of the components of multidimensional series (Lyubushin, 1994). A distinctive feature of function $\lambda_1(\tau, \omega)$ is its response to the presence of those components of a multidimensional series which have the most intense amplitude variations in the considered frequency ω and time τ intervals.

When calculating the statistics $\rho^2(\tau, \omega)$ and $\kappa(\tau, \omega)$ whose values range from 0 to 1, we used the method for constructing the canonical coherences of a multidimensional time series in the moving time window suggested in (Luyubushin, 1998), which is an alternative to the principal component analysis in identifying the synchronization signals.

The frequency-dependent measures of the component-wise canonical coherences $\nu_1(\tau, \omega)$, $\nu_2(\tau, \omega)$, ..., $\nu_l(\tau, \omega)$, where 1, 2,..., l are the numbers of scalar time series composing the l-dimensional time series, describe the degree of coupling of the corresponding scalar components of the multidimensional time series with all the other components. The function

$$\kappa(\tau, \omega) = \nu_1(\tau, \omega)\nu_2(\tau, \omega) \cdot \ldots \cdot \nu_l(\tau, \omega), \qquad (1)$$

as an indicator of the degree of collectiveness in the behavior of the set of considered parameters is highly demanding of the quality of the time series composing the multidimensional series. Its difference from zero means that at a given frequency and in a given time interval all the components of the multidimensional time series are sufficiently strongly coupled with each other, i.e., all the found values $\nu_i(\tau, \omega)$ significantly differ from zero. Otherwise, with any of the factors in (1) being close to zero, the value of $\kappa(\tau, \omega)$ will strongly decrease.

The function

$$\rho^2(\tau, \omega) = \sum_{i=1}^{l} \nu_i^2(\tau, \omega)/l \qquad (2)$$

is more resistant to the inclusion of poorly informative components into the set of the analyzed time series. It is also worth noting that functions $\rho^2(\tau, \omega)$ and $\kappa(\tau, \omega)$, by their construction, mainly depend on the relations between the phases of the components of the multidimensional time series. Therefore, the analysis of their distribution in the frequency-time domain can diagnose the hidden synchronization signals (Lyubushin, 1998).

For constructing the spectral matrices of multidimensional time series, we used the parametric model of the third-order vector autoregression ($p = 3$), which was fitted empirically by trying different models and is optimal.

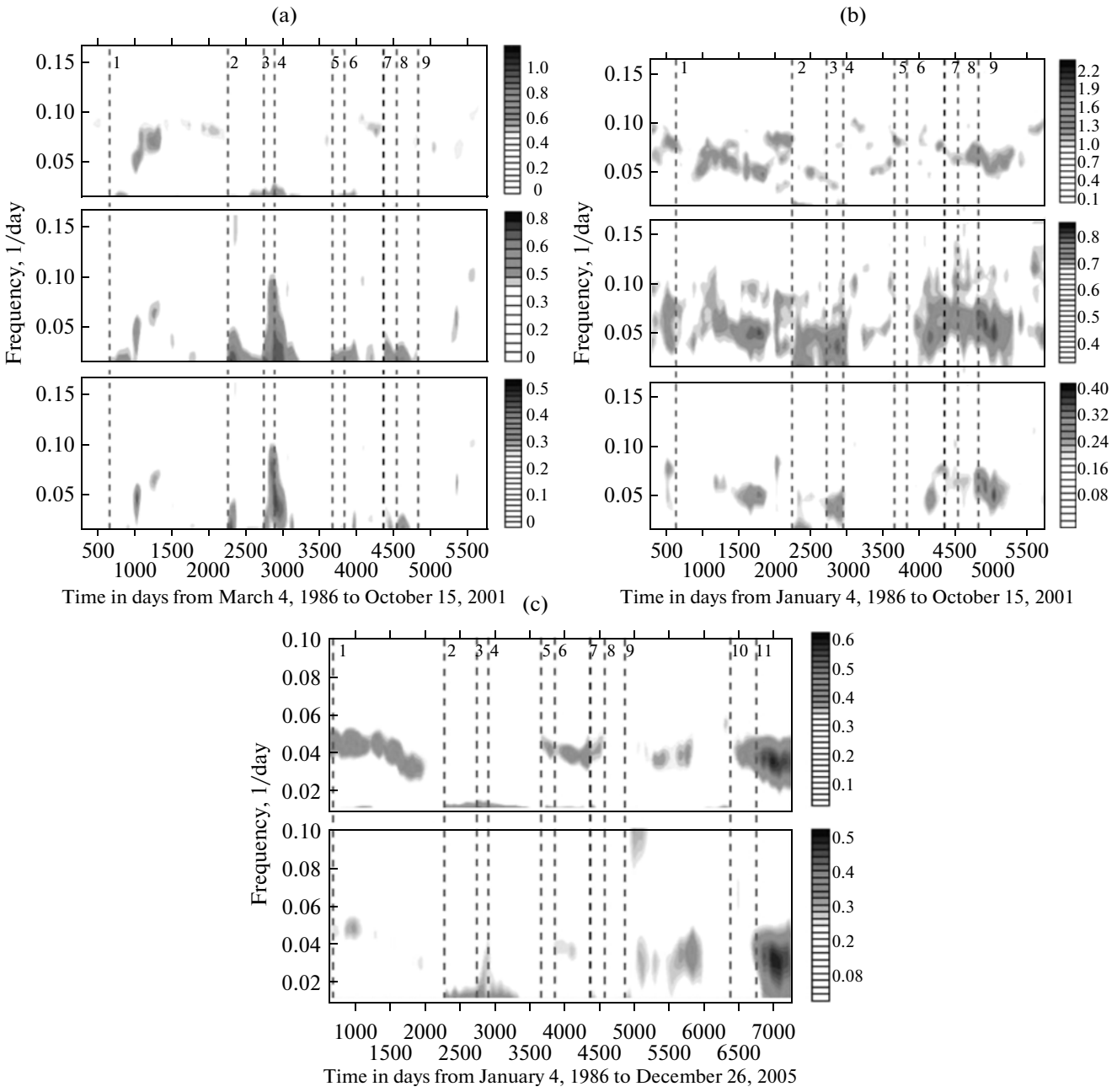

Fig. 4. The examples of the frequency-time diagrams illustrating the evolution of the statistics that characterize the degree of collectiveness in the behavior of the multidimensional time series of hydrogeochemical observations (groups I–III) in comparison to the earthquakes (shown by the vertical dashed lines; the numbers of the earthquakes correspond to Figs. 1 and 2 and the table): (a) I: S1_3 is the three-dimensional time series of the observations at spring 1, the time window is about 300 days in length, and the step is 60 days, from top to bottom: $\lambda_1(\tau, \omega)$, $\rho^2(\tau, \omega)$, $\kappa(\tau, \omega)$; (b) III: the 11-dimensional time series of the concentrations of Cl^-, HCO_3^-, H_4SiO_4 in water of GK1, S1, S2, and M1 sources; the time window is about 300 days in length, the step is 60 days, from top to bottom: $\lambda_1(\tau, \omega)$, $\rho^2(\tau, \omega)$, $\kappa(\tau, \omega)$; (c) II: Cl_3, the time window is about 600 days, the step is 60 days, from top to bottom: $\lambda_1(\tau, \omega)$, $\rho^2(\tau, \omega)$.

THE RESULTS AND DISCUSSION

Figures 4 and 5 show the examples of frequency-time diagrams, which illustrate the evolution of the calculated statistics for multidimensional time series of groups I–III. The synchronization signals are observed in the diagrams as the dark spots corresponding to the increases in the amplitudes of the statistics $\lambda_1(\tau, \omega)$, $\rho^2(\tau, \omega)$, $\kappa(\tau, \omega)$) by at least 50% of their maximal values.

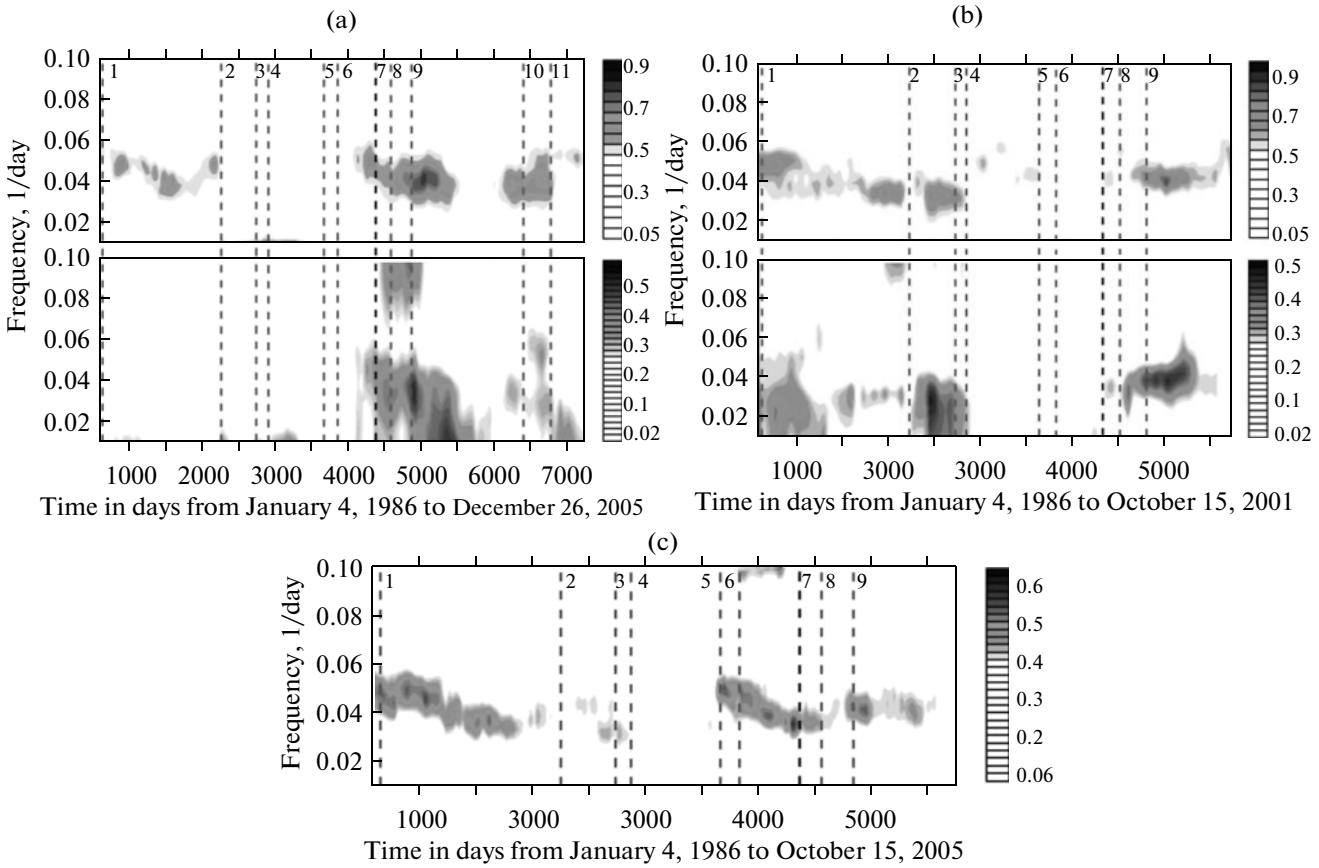

Fig. 5. The frequency-time diagrams of evolution of the statistics characterizing the degree of collectiveness in the behavior of multidimensional time series of hydrogeochemical observations: (a) II: HCO3_4, from top to bottom: $\lambda_1(\tau, \omega)$, $\rho^2(\tau, \omega)$, the time window of 600 days, the step of 60 days; (b) II: H4SiO4_4, from top to bottom: $\lambda_1(\tau, \omega)$, $\rho^2(\tau, \omega)$, the time window of 600 days, the step of 60 days; (c) I: GK1_3, $\lambda_1(\tau, \omega)$, the window of 600 days, the step of 30 days.

Group I time series. In the behavior of S1_3 (Fig. 4a) and S2_3 time series, the signals mainly corresponding to the postseismic effects (P3) are distinguished. These signals are predominantly observed at the periods of ≥ 20–40 days.

The variations in the GK1_3 time series (Fig. 5c) contain long-lasting signals that are traced in 1986–1991, 1996–1997, and 1999 at periods of 15–30 days. These signals can be classified as the effect of the sequential appearance of the precursory and postseismic signals (P2 + P3) from earthquakes 1, 5–8, and 9. Local maxima in the statistics before earthquakes 1–3, 5, 7, and 9 are also identified. These maxima are likely to reflect the relatively short stages of the precursory effects.

Group II time series. Two types of synchronization signals are revealed in the variations of the Cl_3 (Fig. 4c) and HCO3_4 multidimensional time series. The postseismic low-frequency signals at periods ≥30 days (P3) and the signals of relatively higher frequency at periods of 15–25 days are observed in the time windows containing the strongest earthquakes 1–4 and 7. Here, the character of the higher-frequency signals corresponds to a sequential superimposition of the precursory and postseismic effects P2 + P3. For example, the intense P2 signal in the variations of the HCO3_4 time series (Fig. 5a) preceded (during 100 days) the Kronotskoe earthquake of December 5, 1997 (M = 7.8) (no. 7 in the table), and after its occurrence it was changed by the long postseismic signal P3, which shifted towards low frequencies.

The diagram of H4SiO4_4 (Fig. 5b) reflects three long postseismic signals (P3) after earthquakes 1, 2, and 7.

Group III time series. The frequency-time diagrams displaying the evolution of the statistics $\lambda_1(\tau, \omega)$, $\rho^2(\tau, \omega)$, and $\kappa(\tau, \omega)$ for the two multidimensional time series of group III (the example is shown in Fig. 4b) are least informative since they contain lots of poorly expressed synchronization signals, which are difficult to classify by the time of their appearance relative to the considered earthquakes. This is probably due to the increased noise level in the multidimensional time series composed of a large number of scalar time series containing various components of the groundwater chemical composition.

This ambiguity in the appearance of synchronization signals in the variations of multidimensional time series composed of a large number of one-dimensional hydrogeochemical time series may also reflect individual peculiarities of the precursory and postseismic processes in different sources (Kopylova, 2010).

The specific features of the P2 and P3 synchronization signals in the variations of multidimensional time series of groups I and II. The synchronization signals of P2 type identified in the diagrams have a duration from a few dozen days to 100—150 days, averaging 1–3 months, and are observed at periods from 15 days to 30 days. The postseismic signals P3 are longer; they can last for 500 days and even longer and emerge at lower frequencies corresponding to periods from 20 days to 60–120 days. Probably, the P3 synchronization signals can have even longer duration at periods exceeding 60–120 days. However, this frequency-time interval of the synchronization signals in the variations of the hydrogeochemical data is beyond the scope of the present analysis.

We have assessed the stability of the coupling between the synchronization signals P2 and the subsequent strong earthquakes (table). This coupling can be quantified by the following parameter

$$P = m/n, \quad (3)$$

where m is the number of earthquakes before which the diagrams contain the synchronization signals, and n is the total number of earthquakes that occurred during the interval of observations.

For the multidimensional series of groups **I** and **II**, P is estimated to range from 0.4 to 0.7. These values of P correspond to the estimates for the most informative hydrogeochemical parameters such as the changes in the chloride-ion concentration in the water of the GK1 well (Fig. 3, $P = 6/9 = 0.67$) and agree with the estimates of P provided by the other methods (seismological, geodetic, and hydrogeological) ($P = 0.38$–0.75, see Table 4 in (Kopylova and Serafimova, 2009)).

Considered as intermediate-term precursors of the strong earthquakes in Kamchatka, the P2-type synchronization signals have a significant disadvantage: they are difficult or even impossible to distinguish against the background postseismic (P3) signals from previous earthquakes, if both signals develop in close frequency intervals. At the same time, as experience shows, these signals are possible to separate by thoroughly analyzing the frequency-time diagrams reflecting the evolution of all three statistics ($\lambda_1(\tau, \omega)$, $\rho^2(\tau, \omega)$, and $\kappa(\tau, \omega)$) constructed in different moving windows (e.g., 60 and 30 days). As the length of the time window and its time shift decrease, the P2 signal tends to move towards the higher frequency interval.

CONCLUSIONS

The results of analyzing the multidimensional time series of hydrogeochemical observations in relation to the strong ($M \geq 6.6$) earthquakes suggest the following tentative conclusions concerning the prospects of applying the multidimensional analysis technique for processing the hydrogeochemical data for revealing the synchronization signals in their variations.

(1) The synchronization signals in relation to earthquakes mainly appear in the multidimensional time series including the set of one-dimensional series of hydrogeochemical data for a single source (group I) or for a single parameter (group II). The use of all three statistics $\lambda_1(\tau, \omega)$, $\rho^2(\tau, \omega)$, and $\kappa(\tau, \omega)$ identifies such signals unambiguously.

The variations in the S1_3 and S2_3 time series (group I) are typically dominated by the low-frequency postseismic synchronization signals (P3) with periods of ≥20–40 days. In the variations in the GK1_3 time series (Fig. 5c), synchronization signals at the periods of 15–30 days are present in 1986–1991, 1996–1997, and 1999. These signals can be treated as a sequential occurrence of the precursory and postseismic effects (type P2 + P3 signals) in relation to earthquakes 1, 5–8, and 9. Earthquakes 1–3, 5, 7, and 9 are preceded by local maxima in the statistics, which are likely to reflect a relatively short stage of the precursory synchronization P2. Thus, the synchronization signals appeared in variations of the GK1_3 multidimensional time series before six strong earthquakes of the nine seismic events that occurred in 1986–2001 (or in 67% of the cases).

Among the changes in the multidimensional time series Cl_3 (Fig. 4c) and HCO3_4 (Fig. 5a) (group II), two types of synchronization signals are recognized: the postseismic low-frequency P3 signals at periods of at least 30 days and relatively higher frequency signals at periods of 15–25 days. The higher-frequency signals have the character of a sequential superimposition of the precursory and postseismic effects and correspond to the P2 + P3 type. In particular, the intense P2 + P3 synchronization signal first appeared in variations of the HCO3_4 time series a hundred days before the Kronotskoe earthquake of December 5, 1997 ($M = 7.8$) (Fig. 5a).

The variations of the H4SiO4_4 (Fig. 5b) contain three long-lasting postseismic synchronization signals (P3), which are shifted in time relative to earthquakes 1, 2, and 7. These earthquakes significantly affected the observation sites (table). The signals revealed in the behavior of the H4SiO4_4 show that the postseismic changes in the concentrations of silicic acid are mainly hidden and delayed relative to the postseismic changes in the chloride-ion and hydrogen-carbonate ion concentrations.

The multidimensional time series of group III are least informative in the search for synchronization signals. This is due to the increased level of noise components in these time series, which is caused by the different accuracy of analytical determination of separate components in the groundwater composition, as well

as by the local features of the formation of hydrogeoseismic effects in different water sources.

(2) The considered techniques of diagnosing the synchronization signals in the variations of multidimensional time series of the hydrogeochemical data is a useful and sufficiently efficient tool for seismic forecasting. This follows from the estimated correlation between the synchronization signals of type P2 and the subsequent strong earthquakes ($P = 0.4–0.7$) and from the comparison of this type precursor with other intermediate-term precursors currently used for seismic forecasting in Kamchatka, for which P does not exceed 0.75.

ACKNOWLEDGMENTS

The work was supported by the Russian Foundation for Basic Research (grant no. 12-05-00146-a).

REFERENCES

Chebrov, V.N., Saltykov, V.A., and Serafimova, Yu.K., *Prognozirovanie zemletryasenii na Kamchatke. Po materialam raboty Kamchatskogo filiala Rossiiskogo ekspertnogo soveta po prognozu zemletryasenii, otsenke seismicheskoi opasnosti i riska v 1998–2009 gg.* (Forecasting the Earthquakes in Kamchatka. Summarizing the Results of Work of Kamchatka Branch of the Russian Expert Board on Earthquake Prediction and Seismic Hazard and Risk Assessment), Moscow: Svetoch Plyus, 2011.

Khatkevich, Yu.M. and Ryabinin, G.V., Hydrogeochemical studies in Kamchatka, in *Kompleksnye seismologicheskie i geofizicheskie issledovaniya Kamchatki* (Complex Seismological and Geophysical Studies in Kamchatka), Petropavlovsk-Kamchatskii: Kamchatskii pechatnyi dvor, 2004, pp. 96–112.

Kopylova, G.N., Sugrobov, V.M., and Khatkevich, Yu.M., Changes in the behavior of thermal springs and water wells in the Petropavlovsk target area, Kamchatka, as earthquake precursors, *Volcanol. Seismol.*, 1994, vol. 16, no. 2, pp. 145–163.

Kopylova, G.N. and Serafimova, Yu.K., On some medium-term precursors of strong ($M_w \geq 6.6$) earthquakes of Kamchatka in 1987–2004, *Geofizicheskie Issledovaniya*, 2009, vol. 10, no. 4, pp. 17–33.

Kopylova (Grits), G.N., The Effects of Seismicity in the Regime of Groundwater (by the Example of Kamchatka Region), *Extended Abstract of Doct. Sci. (Geol.-Mineral.) Dissertation, Petropavlovsk-Kamchatskii: Kamchatka Branch of the Geophysical Survey, Russian Academy of Science*, 2010.

Kopylova, G.N. and Boldina, S.V., Anomalous changes in chemical composition of groundwater in relation with the Kamchatka earthquake of March 2, 1992 ($M_w = 6.9$), *Geofizicheskie Issledovaniya*, 2012, vol. 13, no. 1, pp. 39–49.

Lyubushin, A.A., Multidimensional analysis of the time series from geophysical monitoring systems, *Fiz. Zemli,* 1993, no. 3, pp. 103–108.

Lyubushin, A.A., Classification of the states of low-frequency geophysical monitoring systems, *Izv. Phys. Solid Earth*, 1995, no. 7/7, pp. 706–702.

Lyubushin, A.A., Kopylova, G.N., and Khatkevich, Yu.M., The use of multivariate analysis for processing groundwater precursors of Kamchatkan earthquakes at the Petropavlovsk site, *Volkanol. Seismol.,* 1996, vol. 18, no. 1, pp. 87–106.

Lyubushin, A.A., Kopylova, G.N., and Khatkevich, Yu.M., Analysis of the spectral matrices of hydrogeological observations at the Petropavlovsk geodynamic research site, Kamchatka, and their comparison with the seismic regime, *Izv. Phys. Solid Earth*, 1997, vol. 33, no. 6, pp. 497–507.

Lyubushin, A.A., Analysis of canonical coherences in the problems of geophysical monitoring, *Izv. Phys. Solid Earth*, 1998, vol. 34, no. 1, pp. 52–58.

Lyubushin, A.A., *Analiz dannykh sistem geofizicheskogo i ekologicheskogo monitoringa* (Analysis of the Data from the Systems of Geophysical and Ecological Monitoring), Moscow: Nauka, 2007.

Serafimova, Yu.K. and Kopylova, G.N., Intermediate-term precursors of large ($M \geq 6.6$) Kamchatka earthquakes for the period from 1987 to 2007: A retrospective assessment of their information content for prediction, *Volcanol. Seismol.*, 2010, vol. 4, no. 4, pp. 223–231.

Sobolev, G.A., *Osnovy prognoza zemletryasenii* (Basics in Earthquake Prediction), Moscow: Nauka, 1993.

Translated by M. Nazarenko